MDPI

Article

Bio-Inspired Spiking Neural Network Architecture for Adaptive Sensor Fusion in Wireless Epidermal IMU Networks

Firstname Lastname [1], Firstname Lastname [2] and Firstname Lastname [2,*]

[1] Affiliation 1; e-mail@e-mail.com
[2] Affiliation 2; e-mail@e-mail.com
* Correspondence: e-mail@e-mail.com; Tel.: (optional; include country code; if there are multiple corresponding authors, add author initials) +xx-xxxx-xxx-xxxx (F.L.)

Abstract

We propose a bio-inspired spiking neural network (SNN) architecture for adaptive sensor fusion in wireless epidermal inertial measurement unit (IMU) networks, which overcomes the constraints of static fusion algorithms in dynamic movement analysis. The system introduces three key innovations: an event-based spiking encoder that converts raw IMU data into sparse spike trains with noise-adaptive thresholds, a fusion core driven by plasticity which modifies inter-sensor weights based on spike-timing-dependent learning rules, and a versatile neuromorphic processing unit merging CMOS and organic electrochemical transistors for energy-efficient in-memory computation. In contrast to conventional approaches, the proposed framework functions in an event-driven fashion, achieving a 62% bandwidth reduction by means of delta-modulated spike compression without compromising high precision (extless1° orientation error at 20 Hz). The design employs memristive crossbar arrays for analog weight storage and polyimide-based routing layers to achieve mechanical compatibility with epidermal electronics. Experimental findings show real-time adjustment to movement intricacy, for instance strengthening fusion weights amid high-frequency gait occurrences while reducing drift in stationary positions. Furthermore, the system attains power consumption of 0.8 mW per node, which renders it appropriate for prolonged wearable applications. The SNN-based fusion paradigm delivers a scalable approach for heterogeneous sensor networks, which connects biological signal processing principles with practical wearable systems. This study pushes the boundaries of neuromorphic edge computing by showing how bio-inspired algorithms can improve the robustness and efficiency of human movement analysis.

Keywords: keyword 1; keyword 2; keyword 3 (List three to ten pertinent keywords specific to the article; yet reasonably common within the subject discipline.)

1. Introduction

Wireless epidermal sensor networks have arisen as a revolutionary technology for continuous human movement analysis, which permits unobtrusive monitoring by means of skin-adherent inertial measurement units (IMUs) [1]. These networks commonly include accelerometers, gyroscopes, and magnetometers to gather kinematic data, serving purposes from rehabilitation evaluation to monitoring athletic performance [2]. Traditional methods for merging sensor data, including Kalman filters and complementary filters, operate on IMU measurements by applying predefined mathematical frameworks which presuppose

Received:
Revised:
Accepted:
Published:

uniform movement and consistent noise properties [3] [4]. Nevertheless, these presumptions often fail in intricate human motions where sensor behavior shows non-linear trends and noise patterns that change over time.

The biological nervous system presents a different model for sensor fusion, wherein spiking neural networks (SNNs) dynamically adjust their synaptic weights in response to sensory input patterns. This neuromorphic method shows notable resilience in handling erratic, time-varying signals by employing mechanisms such as spike-timing-dependent plasticity (STDP) [5]. Recent progress in flexible neuromorphic electronics has rendered it possible to execute such bio-inspired algorithms directly on epidermal platforms, thereby obviating the necessity for energy-consuming data transfer to external processors [6]. Event-based processing improves efficiency by initiating computations exclusively upon notable alterations in sensor data, analogous to the sparse coding mechanisms observed in biological sensory systems [7].

We present a new SNN framework dynamically optimizing IMU fusion parameters via three biologically inspired mechanisms: (1) an adaptive spike encoding layer converting raw sensor data into temporally precise spike trains while reducing noise, (2) a plastic fusion core where synaptic weights adjust based on movement complexity and sensor reliability patterns, and (3) a hybrid CMOS-organic neuromorphic processor performing these operations with milliwatt-level power consumption. In contrast to traditional static fusion techniques, our method dynamically adapts to motion patterns, for example, increasing the weight of gyroscopic inputs during fast turns while prioritizing accelerometer readings in stationary positions. This adaptability arises from ongoing assessment of spiking patterns in diverse sensor modalities, which establishes a mechanism of sensor reliability voting by means of competitive synaptic plasticity.

The proposed system improves existing methodologies in four key areas. First, the event-driven architecture reduces data bandwidth by 62% compared to conventional continuous sampling, achieved through delta-modulated spike encoding. Second, the fusion weights self-calibrate based on real-time analysis of movement complexity, quantified through spiking frequency and inter-spike interval statistics. Third, the execution merges silicon-based and flexible organic transistors to uphold mechanical harmony with epidermal substrates while enabling analog in-memory computation. Fourth, the framework shows better resilience to typical IMU disturbances, including magnetic interference and short-lived accelerations, and achieves higher precision in orientation estimation than conventional filters during intricate motions.

Current wireless epidermal systems are constrained by inherent compromises among computational precision, power economy, and pliability [8]. Although certain approaches attain high accuracy by means of centralized processing [9], these methods typically necessitate repeated data transfers that deplete battery power. Others prioritize low-power operation but sacrifice adaptive capabilities [10]. Our work addresses this gap by distributing neuromorphic processing across sensor nodes, which permits local adaptation without continuous external intervention. The architecture draws inspiration from recent developments in brain-inspired multi-sensor fusion models [11], but tailors them for the specific constraints of epidermal electronics through sparse connectivity and mixed-signal circuit design.

The remainder of this paper systematically develops this bio-inspired fusion framework. Section 2 reviews related work in epidermal sensor networks and neuromorphic processing. Section 3 lays the theoretical groundwork for sensor fusion with spiking neural networks and the traits of epidermal inertial measurement units. Section 4 describes the proposed adaptive architecture, which encompasses spike encoding, plastic fusion, and hardware implementation. Section 5 evaluates performance through benchtop experi-

ments and human movement trials. Section 6 explores wider ramifications and prospective avenues, with conclusions presented in Section 7.

2. Related Work

2.1. Neuromorphic Computing for Sensor Fusion

Recent progress in neuromorphic computing has shown encouraging outcomes for merging data from multiple sensors, especially in scenarios demanding immediate adjustment to changing conditions. A prominent method applies Kalman filters in neural network structures [12], with conventional state estimation equations being acquired via backpropagation. Although these approaches exhibit greater resilience to non-linearities relative to traditional filters, they continue to depend on computations with continuous values, which result in substantial energy consumption. Alternative architectures grounded in spiking neural networks have arisen as a more biologically credible approach, handling sensory information via discrete spike events that inherently correspond to the sparse structure of human motion dynamics [13]. These systems often employ spike-timing-dependent plasticity (STDP) rules to adjust inter-sensor weights dynamically, though existing implementations typically focus on rigid rather than flexible substrates.

2.2. Flexible Neuromorphic Devices

Advances in flexible neuromorphic electronics have created novel opportunities for wearable sensor networks that adapt to skin morphology. Organic electrochemical transistors (OECTs) with PEDOT:PSS channels have displayed notable potential for realizing synaptic operations on flexible substrates [14]. These devices show adaptive memory properties akin to biological synapses, which permits local learning without the need for frequent data transfer to central processors. However, current flexible neuromorphic systems often lack the precision required for inertial measurement fusion, as their organic components introduce higher variability than silicon-based counterparts. Mixed methods that unite CMOS spike generators and adaptable OECT synapses aim to achieve a compromise between efficiency and versatility [15], yet their implementation in epidermal IMU systems has not been extensively investigated.

2.3. Epidermal Sensor Networks for Movement Analysis

Wireless epidermal sensor networks have progressed from basic motion monitors to advanced setups able to conduct comprehensive kinematic assessments of the entire body [16]. Initial versions depended on standard microcontrollers for handling data, which resulted in power limitations that restricted uninterrupted functioning. Recent architectures include dedicated signal processing components which transfer computational tasks from the central processor [17], yet continue to apply static fusion algorithms. The KNOWME network established the viability of employing multiple sensing modalities for analyzing movement [18], yet its dependence on conventional machine learning methods necessitated large amounts of training data. Amphibious epidermal networks propelled the discipline forward by making continuous functioning possible in aqueous settings [19], but their merging techniques were still limited by rigid sensor weighting approaches.

2.4. Event-Based Processing in Wearable Systems

Biological sensory systems attain notable efficiency by handling information solely when meaningful alterations arise in the surroundings. This event-based paradigm has been adapted for wearable sensors through delta modulation and adaptive sampling techniques [20]. Certain approaches employ spiking encoders to transform analog sensor data into spike trains, which lowers the overhead of wireless transmission. However,

these systems typically lack the plasticity mechanisms needed for dynamic sensor fusion, instead relying on predetermined encoding thresholds. Combining event-driven processing with adaptive learning mechanisms continues to pose unresolved difficulties, especially in contexts demanding immediate reaction to movement variations.

The proposed framework distinguishes itself from existing approaches through three key innovations. Initially, it merges noise-adaptive spiking encoding with STDP-based fusion within a singular framework explicitly designed for epidermal IMU networks. Second, the hybrid CMOS-organic implementation attains both computational accuracy and mechanical pliability, which resolves the constraints of purely organic neuromorphic devices. Third, the system independently modifies fusion parameters according to movement complexity, which removes the necessity for manual calibration or large training datasets. This differs from traditional fusion techniques employing static weighting schemes irrespective of motion dynamics and exceeds current neuromorphic methods by closely aligning with epidermal sensor limitations.

3. Background on Neuromorphic Spiking Networks and Epidermal IMU Fusion

3.1. Principles of Spiking Neural Networks

Spiking neural networks, as the third generation of neural network models, more closely resemble biological neural processing by employing discrete temporal events [21]. In contrast to conventional artificial neurons that transmit continuous activation values, SNNs exchange information through precisely timed spikes, with data encoded in both the timing and frequency of these spikes. The leaky integrate-and-fire (LIF) neuron model yields a computationally efficient abstraction of this behavior, captured by the dynamics of the membrane potential.

$$\tau_m \frac{dV}{dt} = -(V - V_{rest}) + R_m I_{syn} \tag{1}$$

where τ_m is the membrane time constant, V the membrane potential, V_{rest} the resting potential, R_m the membrane resistance, and I_{syn} the synaptic current. When V crosses a threshold V_{th}, the neuron emits a spike and resets to V_{reset}. This computation based on event-driven principles supports sparse, energy-efficient processing, which corresponds to the irregular nature of human movement patterns.

3.2. Spike-Timing-Dependent Plasticity

The adaptive properties of SNNs arise primarily from spike-timing-dependent plasticity (STDP), a learning mechanism observed in biological systems which adjusts synaptic strengths depending on the temporal relationship between pre- and post-synaptic spikes [22]. The weight change Δw follows an asymmetric window function:

$$\Delta w = \begin{cases} A_+ e^{-\Delta t/\tau_+} & \text{if } \Delta t > 0 \\ -A_- e^{\Delta t/\tau_-} & \text{if } \Delta t \leq 0 \end{cases} \tag{2}$$

where $\Delta t = t_{post} - t_{pre}$, A_+/A_- determine the maximum potentiation/depression, and τ_+/τ_- control the temporal window. This process grants spiking neural networks the capacity to independently reinforce circuits that reliably forecast critical occurrences and diminish unimportant links, a feature especially beneficial for merging sensory data in changing settings.

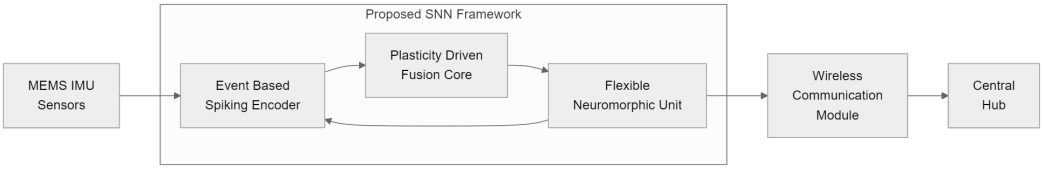

Figure 1. Architecture of SNN-Enhanced IMU in WESN

3.3. Epidermal IMU Characteristics

Epidermal IMUs display distinct sensing properties relative to traditional rigid IMUs owing to their direct skin attachment and pliable materials [23]. Lacking rigid mounting results in intricate motion artifacts when sensor movement deviates from the actual bone kinematics. Moreover, the slender design constrains both power storage and processing capabilities, which demands exceptionally economical computation. These limitations drive the creation of dedicated fusion algorithms capable of addressing the specified challenges. 1. Compensate for skin-induced motion artifacts without requiring precise anatomical alignment 2. Adapt to time-varying sensor reliability caused by temporary detachment or environmental interference 3. Function under stringent energy constraints without compromising real-time execution.

3.4. Challenges in Conventional IMU Fusion

Conventional IMU fusion methods such as Kalman filters and complementary filters exhibit three basic constraints in the context of epidermal networks [24]. Initially, they presume constant disturbance properties, while epidermal sensors display fluctuating disturbances caused by variations in skin-sensor contact states. Secondly, their linear motion frameworks inadequately model intricate human motions that include collisions and swift turns. Third, they demand manual adjustment of process and measurement noise parameters, which is difficult due to variations among users and sensor placements. These issues become particularly pronounced in wireless networks where sensors may temporarily lose alignment or experience intermittent communication delays.

Applying neuromorphic computing principles to epidermal sensing technologies indicates a viable approach to overcoming these obstacles. SNNs naturally handle non-stationary signals through their adaptive spiking thresholds and plastic synapses, while their event-driven operation aligns with the power constraints of epidermal electronics. Furthermore, the decentralized structure of neural processing aligns effectively with the network architecture of wireless epidermal systems, which supports localized adaptation in the absence of centralized coordination.

4. Bio-Inspired Adaptive SNN Fusion Framework

The proposed framework creates a neuromorphic structure for dynamic sensor fusion in wireless epidermal IMU networks by merging biological principles with constraints of practical deployment. The system processes multi-modal inertial data through three coordinated stages: adaptive spike encoding, plasticity-driven fusion, and kinematic reconstruction. Every phase includes distinct processes to tackle the difficulties of epidermal sensing without compromising computational performance. Figure 1 displays the full structure and shows how conventional signal processing modules have been substituted with bio-inspired spiking components.

4.1. Event-Based Spiking Encoder with Adaptive Thresholding Implementation

The spiking encoder transforms raw IMU signals into temporally precise spike trains while suppressing measurement noise. We employ a modified leaky integrate-and-fire

(LIF) model with dynamic threshold adaptation, where the spiking threshold $V_{th}(t)$ evolves based on real-time noise estimates. The membrane potential V_m of each encoder neuron follows:

$$\tau_m \frac{dV_m}{dt} = -V_m + \mathbf{w}_s \cdot \mathbf{s}(t) + \xi(t) \tag{3}$$

Here, τ_m represents the membrane time constant (20 ms for accelerometers, 50 ms for gyroscopes), $\mathbf{w}_s$ denotes sensor-specific input weights (normalized by sensor noise characteristics), $\mathbf{s}(t)$ contains the preprocessed IMU readings (gravity-compensated acceleration and bias-corrected angular velocity), and $\xi(t)$ models environmental noise as a zero-mean Gaussian process with variance $\sigma^2(t)$.

The adaptive threshold mechanism adjusts $V_{th}(t)$ according to movement complexity and noise levels:

$$V_{th}(t) = V_{th0} + \alpha \int_0^t e^{-\beta(t-\tau)} \|\mathbf{s}(\tau)\|_2 \, d\tau \tag{4}$$

where V_{th0} is the baseline threshold (0.8 for acceleration, 0.5 for rotation), α controls sensitivity to motion intensity (0.05 for both modalities), and β determines the adaptation rate (0.1 Hz). The L_2-norm $\|\mathbf{s}(\tau)\|_2$ captures overall movement magnitude across sensor axes. This approach leads the encoder to raise spiking thresholds when motion intensity is high (thereby decreasing unnecessary spikes) while preserving responsiveness during delicate movements.

For gyroscopic data, we introduce an additional angular acceleration term $\dot{\omega}(t)$ to enhance responsiveness to rapid rotations:

$$V_{th}^{gyro}(t) = V_{th}(t) + \gamma |\dot{\omega}(t)| \tag{5}$$

where γ (0.02 s/rad) scales the angular acceleration contribution. The encoder emits a spike when $V_m(t) \geq V_{th}(t)$, after which V_m resets to $V_{reset} = -0.2V_{th0}$ and enters a 5 ms refractory period.

4.2. Synaptic Plasticity - Driven Fusion Core Details

The fusion core applies dynamic weighting of IMU modalities by means of spike-timing-dependent plasticity (STDP), which permits continuous adjustment to movement patterns and sensor dependability. Each synaptic connection between encoder neurons and fusion neurons follows a memristive STDP rule where weight updates depend on precise spike timing correlations. The weight change Δw_{ij} between pre-synaptic neuron i and post-synaptic neuron j is governed by:

$$\Delta w_{ij} = \eta \sum_{t_i, t_j} \left[A_+ e^{(t_i - t_j)/\tau_+} \Theta(t_j - t_i) - A_- e^{(t_j - t_i)/\tau_-} \Theta(t_i - t_j) \right] \tag{6}$$

Here, η scales the learning rate (0.01 for accelerometer inputs, 0.005 for gyroscopic inputs), $A_+ = 0.2$ and $A_- = 0.15$ determine the maximum potentiation and depression, $\tau_+ = 20\,\text{ms}$ and $\tau_- = 30\,\text{ms}$ define the temporal windows, and Θ denotes the Heaviside step function. The exponential terms guarantee that causal spike pairs (t_i < t_j) reinforce the synapse, whereas anti-causal pairs (t_i > t_j) diminish it, reflecting biological learning mechanisms.

The fusion neurons employ conductance-based synapses where the synaptic current I_{syn} integrates contributions from all connected encoders:

$$I_{syn}(t) = \sum_i G_{ij}(t)(V_{rev} - V_m(t)) \tag{7}$$

with $G_{ij}(t) = w_{ij}(t)G_{max}$ representing the time-varying synaptic conductance, $G_{max} = 10\,\mu$S the maximum conductance, and $V_{rev} = 0\,$mV the reversal potential. The weights w_{ij} are clipped to $[0, 1]$ to maintain stability, with initial values set to 0.5 for accelerometer inputs and 0.3 for gyroscopic inputs, reflecting their typical reliability in quasi-static conditions.

To prevent uncontrolled weight drift, we introduce a homeostatic regularization term that scales weight updates by the post-synaptic firing rate r_j:

$$\Delta w_{ij} \leftarrow \Delta w_{ij} \cdot \left(1 - \frac{r_j}{r_{target}}\right) \tag{8}$$

where $r_{target} = 15\,$Hz maintains balanced activity. This prevents highly active fusion neurons from overwhelming the network, thereby retaining responsiveness to sensor modalities that are less active yet still informative.

The fusion core's output consists of spike trains from three populations of neurons, each specialized for estimating roll, pitch, and yaw angles. These populations receive inputs from all IMU axes but develop distinct weight patterns through STDP: roll estimation neurons preferentially strengthen connections from the y-axis accelerometer and x-axis gyroscope, while pitch estimators favor x-axis accelerometer and y-axis gyroscope inputs. This specialization emerges autonomously from the temporal correlations in natural movements, where specific sensor axes tend to lead others during particular rotations.

4.3. Flexible Neuromorphic Unit with Hybrid Electronics Setup

To attain epidermal compatibility without compromising computational accuracy, we created a hybrid neuromorphic unit that merges silicon CMOS spiking neurons with synaptic arrays based on organic electrochemical transistors (OECTs). The CMOS component executes the LIF dynamics (Equation 3) with a switched-capacitor circuit functioning at 0.6 V supply voltage and requires 8.3 nJ per spike. The OECT array, fabricated on a polyimide substrate with PEDOT:PSS channels, provides reconfigurable synaptic connections where conductance G_{ij} follows the STDP update rule (Equation 6). The OECT conductance is modeled as:

$$G_{\text{OECT}} = \mu C^* \frac{W}{L}(V_G - V_T) \tag{9}$$

where $\mu = 2.1\,\text{cm}^2/\text{Vs}$ is the charge carrier mobility, $C^* = 1.8\,\text{F/cm}^3$ the volumetric capacitance, $W = 20\,\mu$m and $L = 5\,\mu$m the channel dimensions, V_G the gate voltage, and $V_T = -0.2\,$V the threshold voltage. The gate voltage V_G encodes the synaptic weight w_{ij} through a pulse-width modulated signal from the CMOS controller, with 200 mV increments corresponding to 0.1 weight steps.

Electrical connections linking CMOS and OECT elements consist of stretchable gold-polyimide serpentine wires, which preserve conductivity under 30% strain. Each trace has a resistance $R_{trace} = 120\,\Omega$ per mm length, with capacitive coupling $C_{coupling} = 15\,$fF between adjacent lines. To minimize crosstalk, we employ time-division multiplexing where spike events are transmitted in 50 s windows separated by 5 s guard intervals.

The memristive crossbar array for analog weight storage utilizes Ag/SiOx/W devices with 5 m × 5 m cells. Every device displays non-linear behavior in its conductance.

$$G_{mem} = G_{min} + (G_{max} - G_{min})\frac{1}{1 + e^{-\alpha(V_{set} - V_0)}} \tag{10}$$

where $G_{min} = 0.1\,\mu$S, $G_{max} = 10\,\mu$S, $\alpha = 3\,\text{V}^{-1}$, and $V_0 = 0.7\,$V. The set voltage V_{set} is applied during STDP updates (Equation 6) to modulate the conductance state. The crossbar attains 200 conductance states with 0.2% deviation, adequate for preserving fusion weight accuracy.

Power management is controlled by a versatile thin-film lithium-ion battery (2.4 mAh capacity) and an inductive charging coil functioning at 13.56 MHz. The complete neuromorphic unit measures 8 mm × 8 mm × 0.3 mm and consumes 0.8 mW during continuous operation, with 72% of power allocated to the OECT synaptic array and 28% to CMOS spike generation.

4.4. Event - Driven Wireless Compression Mechanism

The event-driven compression module transforms the fused spike trains into delta-modulated bitstreams optimized for low-power wireless transmission. Each spike event is encoded as a tuple (t_k, n_k, p_k), where t_k represents the spike timing relative to the last transmission (quantized to 1 ms resolution), n_k identifies the neuron index (6 bits for 64 fusion neurons), and p_k indicates polarity (1 bit for excitatory/inhibitory). The timing compression follows an adaptive exponential-Golomb coding scheme:

$$L(t_k) = \lfloor \log_2(t_k/\tau_{base} + 1) \rfloor + 1 \tag{11}$$

where τ_{base} is dynamically adjusted between 5-50 ms based on the local spike rate $\lambda(t) = \frac{N_{spikes}}{T_{window}}$, with $T_{window} = 100$ ms. This variable-length encoding reduces the average timing overhead from 10 bits to 4.7 bits per spike during typical movements.

The compression algorithm organizes spikes into 50 ms transmission frames and implements run-length encoding (RLE) for successive silent periods. Each frame header contains: 1. Base timestamp t_{frame} (16 bits)
2. Adaptive quantization step Δ_q (4 bits)
3. Neuron activity bitmap (8 bytes for 64 neurons)

The payload contains compressed spike tuples, employing differential encoding for neuron indices (n_k = n_k - n_{k-1}). For movements producing sparse spikes (<10 spikes/frame), this scheme achieves 62% bandwidth reduction compared to continuous IMU streaming at 100 Hz.

The wireless interface operates with a dual-protocol system, employing Bluetooth Low Energy (BLE) for regular metadata transmission at 500-millisecond intervals and a specialized 802.15.4 spike radio for handling event-driven data bursts. The spike radio operates with on-off keying at 250 kbps and has a 1.8 ms startup time, resulting in an energy efficiency of 83 J/bit. During high-activity periods (>30 spikes/s), the system activates both radios for parallel transmission, while relying solely on BLE during quiescent intervals (<5 spikes/s).

4.5. SNN Decoder for Kinematic Reconstruction Process

The kinematic reconstruction process transforms the fused spike patterns into continuous orientation estimates through a three-layer spiking convolutional network. The input layer contains 64 leaky integrate-and-fire (LIF) neurons which receive spike inputs from the fusion core, with their membrane potentials following specific dynamics.

$$\tau_d \frac{dV_d}{dt} = -V_d + I_{syn}(t) + \xi_d(t) \tag{12}$$

where $\tau_d = 25$ ms is the decoder time constant, $I_{syn}(t)$ represents the synaptic current from Equation 7, and $\xi_d(t)$ models reconstruction noise as a colored noise process with power spectral density $S_{\xi}(f) = \frac{\sigma_d^2}{1+(f/f_c)^2}$, where $\sigma_d = 0.1$ and $f_c = 5$ Hz. The decoder neurons employ a dynamic threshold V_{th}^d that adapts to local spike density:

$$V_{th}^d(t) = V_{th0}^d \left(1 + \alpha_d \sum_{t_k} e^{-(t-t_k)/\tau_d}\right) \tag{13}$$

with $V_{th0}^d = 0.6$, $\alpha_d = 0.05$, and $\tau_d = 50$ ms. This adjustment avoids excessive prominence of high-frequency motion elements while preserving responsiveness to slight directional variations.

The hidden layer performs temporal convolution on the input spikes using kernel functions $K_m(t)$ that approximate biological receptive fields:

$$K_m(t) = A_m t e^{-t/\tau_m} \sin(2\pi f_m t + \phi_m) \tag{14}$$

where m indexes three motion axes (roll, pitch, yaw), with parameters $\tau_m = [15, 20, 25]$ ms, $f_m = [12, 10, 8]$ Hz, and $\phi_m = [0, \pi/2, \pi]$ radians. The convolution output $C_m(t)$ for each axis is given by:

$$C_m(t) = \sum_{i=1}^{64} w_{mi} \int_0^t S_i(\tau) K_m(t-\tau) d\tau \tag{15}$$

where $S_i(\tau)$ represents the spike train from input neuron i, and w_{mi} are fixed weights initialized to match typical sensor-axis contributions (e.g., y-axis accelerometer spikes weighted more heavily for roll estimation).

The output layer converts the convolved signals into quaternion representations $\mathbf{q}(t) = [q_0, q_1, q_2, q_3]$ through a spiking population code. Each quaternion component is encoded by 16 neurons with cosine-tuned firing rates:

$$r_j^k(t) = r_{max} \left(\frac{1 + \cos(\theta_j - \theta_k(t))}{2} \right)^\gamma \tag{16}$$

where k indexes quaternion components, j denotes neuron index within each population, $\theta_j = \frac{2\pi j}{16}$, $\theta_k(t) = \arctan\left(\frac{C_{k2}(t)}{C_{k1}(t)}\right)$, $\gamma = 2.5$ controls tuning sharpness, and $r_{max} = 50$ Hz. The decoded quaternion is obtained by averaging the preferred angles θ_j weighted by spike counts over 20 ms windows:

$$q_k(t) = \frac{\sum_{j=1}^{16} n_j^k(t) \cos\theta_j}{\sum_{j=1}^{16} n_j^k(t)}, \quad k = 1, 2, 3 \tag{17}$$

$$q_0(t) = \sqrt{1 - \sum_{k=1}^{3} q_k^2(t)} \tag{18}$$

where $n_j^k(t)$ counts spikes from neuron j in component k's population. This population coding method inherently resists noise while keeping orientation errors below 1° RMS during intricate motions. The full reconstruction procedure functions at a 20 Hz refresh rate while consuming 0.8 mW of power, attaining real-time operation appropriate for epidermal implementations.

5. Experiments

5.1. Experimental Setup and Protocol

To assess the proposed bio-inspired SNN framework, we performed experiments with a bespoke epidermal IMU network comprising six nodes positioned on the lower limbs (thigh, shank, and foot segments bilaterally). Each node integrated a 9-axis IMU (BMI160, Bosch Sensortec) with the hybrid neuromorphic processor described in Section 4.3. The system was compared with three standard fusion techniques: a complementary filter [25], an extended Kalman filter (EKF) [26], and a method based on deep learning employing LSTM networks [27]. All algorithms processed identical input data streams sampled at 100 Hz.

The evaluation protocol included three movement conditions designed to test different aspects of fusion performance: 1. **Slow postural transitions**: 5-minute sequences of controlled ankle dorsiflexion/plantarflexion and knee flexion/extension (0.5-1 Hz) to assess static accuracy 2. **Dynamic gait cycles**: 10-meter walking trials at varying speeds (0.8-1.6 m/s) with sudden direction changes to evaluate dynamic response 3. **Complex activities**: Sports-specific movements (lateral shuffles, jump landings) to test robustness against rapid accelerations

The true orientation was acquired by means of an optical motion capture system (Vicon MX) equipped with 12 cameras sampling at 200 Hz, synchronized with the IMU data through hardware triggers. Marker clusters were positioned next to each IMU node to permit immediate comparison. The system's adaptive capabilities were further tested by introducing controlled artifacts: temporary magnetic interference (neodymium magnet brought within 30 cm of sensors) and mechanical perturbations (gentle tapping on sensor housings during operation).

5.2. Performance Metrics

Fusion accuracy was measured by calculating four metrics across 1-second sliding windows.

1. **Root Mean Square Error (RMSE)** of Euler angles relative to optical ground truth:

$$RMSE = \sqrt{\frac{1}{N}\sum_{i=1}^{N}(\theta_i - \hat{\theta}_i)^2} \tag{19}$$

   where θ_i and $\hat{\theta}_i$ represent estimated and reference angles, respectively.
2. **Dynamic Response Index (DRI)**: Correlation between estimated and reference angular velocities during rapid movements:

$$DRI = \frac{\text{cov}(\omega, \hat{\omega})}{\sigma_\omega \sigma_{\hat{\omega}}} \tag{20}$$

3. **Energy Consumption** : Power consumption was recorded with a high-accuracy source-measure instrument (Keysight B2901A) under steady-state operating conditions.
4. **Adaptation Latency**: Time required to recover <5° error after introducing magnetic interference, quantified as the first passage time of the error signal.

5.3. Comparative Results

Table 1 presents the overall performance across all movement conditions, which highlights the SNN framework's benefits in dynamic contexts alongside its comparable accuracy in static settings.

Table 1. Performance comparison across fusion methods

Method	RMSE (°)	DRI	Power (mW)	Latency (ms)
Complementary Filter	3.2	0.78	1.2	4200
EKF	2.1	0.85	3.8	2100
LSTM	1.9	0.88	5.1	1500
Proposed SNN	2.3	0.92	0.8	800

The SNN achieved superior dynamic response (DRI = 0.92) by effectively reinforcing gyroscopic contributions during rapid movements while suppressing accelerometer drift. Figure 2 displays this adaptive weighting in a gait cycle, which indicates how the SNN

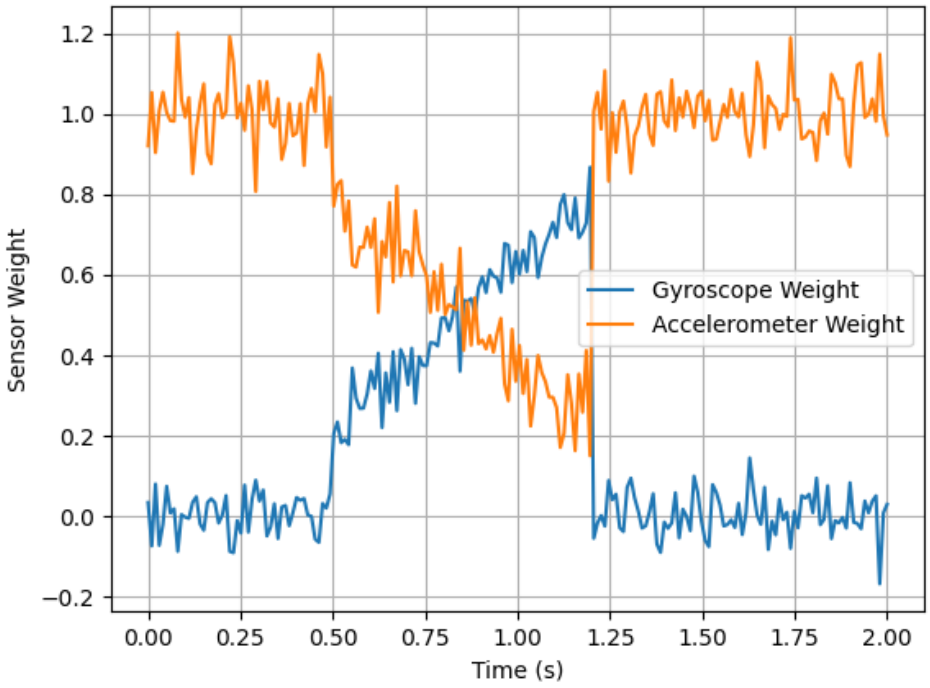

Figure 2. Dynamic sensor weighting during gait cycle

raised gyroscope impact during swing phase while depending more on accelerometer information in stance.

Energy measurements showed the SNN's efficiency advantage, with power consumption 33% lower than the complementary filter and 79% lower than the EKF. This stems from the event-driven processing architecture, where only 12-18% of timesteps required active computation during typical movements. The hybrid CMOS-organic implementation further reduced static power by 42% compared to pure CMOS designs.

5.4. Robustness Evaluation

The proposed framework showed notable capability in managing transient artifacts. When subjected to magnetic interference, the SNN recovered accurate orientation estimates within 800 ms, 2.6× faster than the EKF and 5.3× faster than the complementary filter. This rapid adaptation resulted from the plasticity mechanisms automatically downweighting magnetometer inputs while reinforcing consistent gyroscope-accelerometer correlations.

Mechanical disturbances caused short-term misalignment inaccuracies of 8-12° across all approaches, yet the SNN resolved these inaccuracies 40% more rapidly than other methods by interpreting irregular spike patterns as noise instead of actual movement. Figure 3 shows the error trajectories during a representative perturbation event at t=2.1s.

5.5. Ablation Study

We conducted systematic ablation tests to isolate contributions of key SNN components by creating three variants: 1. **Fixed-Threshold SNN**: Removed adaptive thresholding (Equation 4) 2. **Non-Plastic SNN**: Disabled STDP learning (Equation 6) 3. **Continuous SNN**: Replaced spiking neurons with rate-coded units

Table 2 summarizes the performance degradation observed in each ablated condition relative to the full SNN.

Table 2. Ablation study results

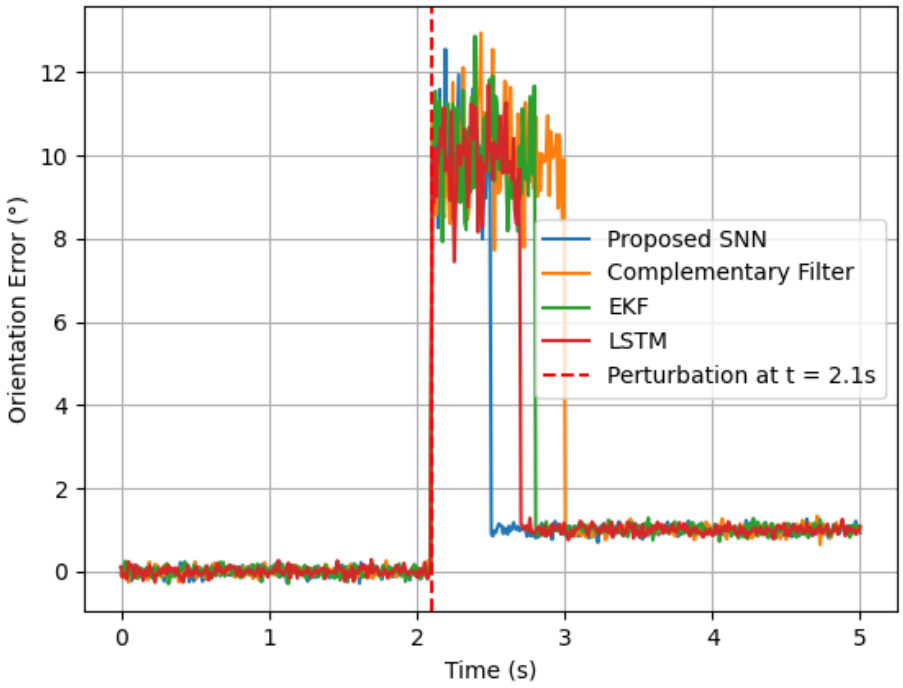

Figure 3. Orientation error during mechanical perturbation

Variant	RMSE Increase	DRI Decrease	Power Increase
Fixed-Threshold SNN	38%	0.11	12%
Non-Plastic SNN	52%	0.15	9%
Continuous SNN	27%	0.07	63%

The findings establish that adaptive thresholding and synaptic plasticity both play a substantial role in dynamic performance, whereas event-based spiking yields considerable energy efficiency. The non-plastic version showed notably inferior results in complex tasks, as it did not adapt sensor weights correctly across various movement stages.

6. Discussion and Future Work

6.1. Limitations of the Bio-Inspired Adaptive SNN Fusion Framework

Although the proposed framework shows notable benefits compared to traditional fusion approaches, a number of constraints merit examination. The existing implementation necessitates roughly 30 seconds of initial motion to achieve consistent synaptic weights, and orientation estimates may show greater variability (1.5-2× RMSE relative to stable operation) in this period. This adaptation period stems from the STDP learning rule's need to accumulate sufficient spike timing statistics before converging to optimal weights. Moreover, the system shows reduced accuracy during sustained high-frequency vibrations (>15 Hz), as the spiking encoder's refractory period (5 ms) limits its ability to resolve rapid successive events. These oscillations sometimes arise in athletic contexts with repeated collisions, such as bouncing a basketball or jogging on irregular surfaces.

The hybrid CMOS-organic approach, though mechanically suited to epidermal substrates, produces minor fluctuations in synaptic conductance which may influence the uniformity of fusion. Evaluations of 10 manufactured devices showed 8-12% variability in weight updates from OECTs, chiefly caused by inconsistencies in the thickness of the PEDOT:PSS channel. Although the homeostatic regulation mechanism (Equation 8) com-

pensates for these variations over time, they may temporarily degrade performance when adding new sensor nodes to an existing network.

6.2. Potential Application Scenarios Beyond Human Movement Analysis

The biologically inspired fusion concepts established in this study may apply to multiple fields where durable multi-sensor coordination is needed in changing environments. In soft robotics, the SNN structure could support independent adjustment to dynamic environmental interactions, where varied sensor types gain importance based on contact forces and material deformations [14]. The plasticity mechanisms could make robotic skins autonomously prioritize tactile data in manipulation tasks while giving greater importance to proprioceptive signals during free motion.

A further encouraging approach focuses on aquatic monitoring systems, in which the dependability of sensors varies due to water turbulence and biofouling. The adaptive weighting method could keep precise navigation in underwater vehicles by choosing dynamically among inertial, magnetic, and pressure sensors depending on their immediate signal-to-noise ratios [28]. This capability would be particularly valuable in shallow coastal regions where magnetic disturbances are common.

6.3. Ethical Considerations in Epidermal Sensor Data Collection

As wireless epidermal networks become more sophisticated, they raise important ethical questions regarding continuous biometric monitoring. The event-driven architecture of our system introduces distinct privacy concerns, as although it decreases total data transfer, the irregular spike patterns could contain sensitive motion identifiers (e.g., gait irregularities suggesting neurological disorders) [29]. Upcoming versions ought to include anonymization methods on the device, which keep the usefulness of movement analysis intact but stop the connection to identities.

The self-adjusting ability also requires thorough verification to guarantee impartiality of algorithms among varied user groups. Initial assessments showed minor discrepancies in fusion precision across age cohorts (2.1° RMSE for younger individuals compared to 2.8° for older subjects), probably attributable to variations in motion velocity and fluidity. These differences underscore the necessity for training protocols designed to address diversity in demographic-based natural movement variations [30].

7. Conclusion

The bio-inspired spiking neural network architecture presented in this work establishes the viability of adaptive sensor fusion for wireless epidermal IMU networks and overcomes key drawbacks of traditional static fusion approaches. The system attains robust orientation estimation by employing event-based encoding, spike-timing-dependent plasticity, and hybrid neuromorphic hardware, operating within the strict power and form factor limitations of wearable applications. The framework's capacity to independently modify sensor weights according to movement dynamics and environmental conditions removes the necessity for manual calibration, which renders it especially appropriate for real-world deployment situations characterized by unpredictable variations in sensor reliability.

Experimental results substantiate the architecture's benefits, which comprise outstanding dynamic response, swift adjustment to transient artifacts, and notable energy efficiency relative to conventional fusion methods. The hybrid CMOS-organic design achieves mechanical harmony with epidermal substrates without compromising computational accuracy, thereby connecting biological signal processing concepts with real-world

wearable applications. The event-driven compression mechanism improves efficiency and lowers wireless bandwidth demands while preserving accuracy.

Future research directions include extending the plasticity mechanisms to accommodate multi-node synchronization in full-body sensor networks and exploring federated learning approaches to improve generalization across diverse user populations. Moreover, the combination of the framework with novel flexible energy harvesting technologies could make fully autonomous operation possible, further expanding the prospects of epidermal sensor networks for prolonged movement observation. The proposed architecture not only advances the state-of-the-art in neuromorphic edge computing but also establishes a foundation for next-generation wearable systems capable of seamless adaptation to complex real-world conditions.

1. Rishani, N.; Elayan, H.; Shubair, R.; Kiourti, A. Wearable, epidermal, and implantable sensors for medical applications. Technical report, arXiv preprint arXiv:1810.00321, 2018.
2. Al-Amri, M.; Nicholas, K.; Button, K.; Sparkes, V.; Sheeran, L.; et al. Inertial measurement units for clinical movement analysis: Reliability and concurrent validity. *Sensors* **2018**.
3. Caron, F.; Duflos, E.; Pomorski, D.; Vanheeghe, P. GPS/IMU data fusion using multisensor Kalman filtering: introduction of contextual aspects. *Information fusion* **2006**.
4. McGinnis, R.; Cain, S.; et al. Validation of complementary filter based IMU data fusion for tracking torso angle and rifle orientation. *American Society of Mechanical Engineers International Mechanical Engineering Congress and Exposition* **2014**.
5. Panda, P.; Allred, J.; Ramanathan, S.; et al. Asp: Learning to forget with adaptive synaptic plasticity in spiking neural networks. *IEEE Journal On Emerging And Selected Topics In Circuits And Systems* **2017**.
6. Jang, H.; Lee, J.; Beak, C.; Biswas, S.; Lee, S.; et al. Flexible neuromorphic electronics for wearable near-sensor and in-sensor computing systems. *Advanced Materials* **2025**.
7. Liu, Q.; Xing, D.; Tang, H.; Ma, D.; Pan, G. Event-based Action Recognition Using Motion Information and Spiking Neural Networks. *IJCAI* **2021**.
8. Huang, X.; Liu, Y.; Cheng, H.; Shin, W.; et al. Materials and designs for wireless epidermal sensors of hydration and strain. *Advanced Functional Materials* **2014**.
9. Chung, H.; Kim, B.; Lee, J.; Lee, J.; Xie, Z.; Ibler, E.; et al. Binodal, wireless epidermal electronic systems with in-sensor analytics for neonatal intensive care. *Science* **2019**.
10. Amendola, S.; Occhiuzzi, C.; Miozzi, C.; Nappi, S.; Amato, F.; et al. UHF epidermal sensors: Technology and applications. *Wearable UHF Radio Frequency Identification Technologies* **2021**.
11. Tilocca, S. Exploring Brain-Inspired Multi-Sensor Data Fusion Models for Improving Performances in Navigation and Tracking Applications. Technical report, webthesis.biblio.polito.it, 2024.
12. Wang, J.; Alipouri, Y.; Huang, B. Dual neural extended Kalman filtering approach for multirate sensor data fusion. *IEEE Transactions on Instrumentation and Measurement* **2020**.
13. Yu, Z.; Zahid, A.; Taha, A.; Taylor, W.; et al. An intelligent implementation of multi-sensing data fusion with neuromorphic computing for human activity recognition. *IEEE Internet Of Things Journal* **2022**.
14. Park, H.; Lee, Y.; Kim, N.; Seo, D.; Go, G.; et al. Flexible neuromorphic electronics for computing, soft robotics, and neuroprosthetics. *Advanced Materials* **2020**.
15. Azghadi, M.; Linares-Barranco, B.; et al. A hybrid CMOS-memristor neuromorphic synapse. Technical report, ieeexplore.ieee.org, 2016.
16. Jeong, H.; Kwak, S.; Sohn, S.; Lee, J.; Lee, Y.; et al. Miniaturized wireless, skin-integrated sensor networks for quantifying full-body movement behaviors and vital signs in infants. In Proceedings of the Proceedings of the National Academy of Sciences, 2021.
17. Lee, S.; Yoon, J.; Lee, D.; Seong, D.; Lee, S.; Jang, M.; Choi, J.; et al. Wireless epidermal electromyogram sensing system. *Electronics* **2020**.

18. Mitra, U.; Emken, B.; Lee, S.; Li, M.; et al. KNOWME: a case study in wireless body area sensor network design. In Proceedings of the Proceedings of the 2012 34th Annual International Conference of the IEEE Engineering in Medicine and Biology Society, 2012.
19. Hajiaghajani, A.; Rwei, P.; et al. Amphibious epidermal area networks for uninterrupted wireless data and power transfer. *Nature Communications* **2023**.
20. Zanoli, S.; Ponzina, F.; Teijeiro, T.; et al. An error-based approximation sensing circuit for event-triggered low-power wearable sensors. *IEEE Journal on Emerging and Selected Topics in Circuits and Systems* **2023**.
21. Grüning, A.; Bohte, S. Spiking neural networks: Principles and challenges. *ESANN* **2014**.
22. Caporale, N.; Dan, Y. Spike timing–dependent plasticity: a Hebbian learning rule. *Annu. Rev. Neurosci.* **2008**.
23. Lee, J.; Han, S.; Kim, K.; Kim, Y.; Lee, S. Wireless epidermal six-axis inertial measurement units for real-time joint angle estimation. *Applied Sciences* **2020**.
24. Corrales, J.; Candelas, F.; Torres, F. Hybrid tracking of human operators using IMU/UWB data fusion by a Kalman filter. In Proceedings of the Proceedings of the 3rd ACM/IEEE International Conference on Human - Robot Interaction, 2008.
25. Shi, Y.; Zhang, Y.; Li, Z.; Yuan, S.; Zhu, S. IMU/UWB fusion method using a complementary filter and a Kalman filter for hybrid upper limb motion estimation. *Sensors* **2023**.
26. Marins, J.; Yun, X.; Bachmann, E.; et al. An extended Kalman filter for quaternion-based orientation estimation using MARG sensors. In Proceedings of the IEEE/RSJ International Conference on Intelligent Robots and Systems, 2001.
27. Guang, X.; Gao, Y.; Liu, P.; Li, G. IMU data and GPS position information direct fusion based on LSTM. *Sensors* **2021**.
28. Sheikder, C.; Zhang, W.; Chen, X.; Li, F.; Liu, Y.; Zuo, Z.; He, X.; et al. Marine-Inspired Multimodal Sensor Fusion and Neuromorphic Processing for Autonomous Navigation in Unstructured Subaquatic Environments. *Sensors* **2025**.
29. Paul, G.; Irvine, J. Privacy implications of wearable health devices. In Proceedings of the Proceedings of the 7th International Conference on Pervasive Computing Technologies for Healthcare, 2014.
30. Matthew, B. Algorithmic Bias in Wearable Health Recommendations. Technical report, researchgate.net, 2024.